T. Brattberg
Ph.D. Student.

H. Chanson
Senior Lecturer,
Fluid Mechanics, Hydraulics and
Environmental Engineering.

L. Toombes
Ph.D. Student.

Department of Civil Engineering,
The University of Queensland,
Brisbane QLD 4072,
Australia

Experimental Investigations of Free-Surface Aeration in the Developing Flow of Two-Dimensional Water Jets

Turbulent water jets discharging into the atmosphere are often characterized by a substantial amount of free-surface aeration. The effects can be detrimental or beneficial. In any case, the knowledge of the air entrainment mechanisms is essential for an optimum design. New experimental data are presented in the developing flow region of two-dimensional water jets discharging into air. The results indicate that the air diffusion takes place rapidly downstream of the nozzle and it is nearly independent of the momentum transfer process. Further, the distribution of air bubble frequency may be related to the air content distribution by a parabolic relationship.

Accuracy

The error on the positions $\{x, y, z\}$ of the probes was less than:

	Δx	Δy	Δz
Experiment No. 1:	<1 cm	<0.025 mm	<1 mm
Experiment No. 2:	<1 cm	<0.025 mm	<1 mm
Experiment No. 3:	<0.1 mm	<0.1 mm	<1 mm

The error on the discharge measurement was less than 2%.

The error on the air concentration (void fraction) measurements was estimated as: $\Delta C/C = 2\%$ for $5 < C < 95\%$, $\Delta C/C = 0.001/(1 - C)$ for $C > 95\%$, and $\Delta C/C = 0.001/C$ for $C < 5\%$.

The accuracy of the clear-water velocity data was normally estimated as: $\Delta V/V = 1\%$.

The error on the mean air-water velocity measurements was estimated as: $\Delta V/V = 5\%$ for $5 < C < 95\%$.

The minimum detectable bubble chord length was about 200 μm in a 2 m/s flow and 80 μm in a 8 m/s jet based upon a data acquisition frequency of 10 kHz per channel.

Introduction

Turbulent water jets discharging into the atmosphere are often characterized by a substantial amount of free-surface aeration. Applications include water jets at bottom outlets to dissipate energy, jet flows downstream of a spillway ski jump, mixing devices in chemical plants and spray devices, water jets for fire-fighting, jet cutting (e.g., coal mining) and with Pelton turbines. A related case is the ventilated cavity flow, observed downstream of blunt bodies, on the extrados of foils and turbine blades and on spillways (i.e., aeration devices).

The effects of air entrainment can be detrimental (e.g., loss of jet momentum) or beneficial (e.g., mixing enhancement). In any case, knowledge of the air entrainment mechanisms is essential for an optimum design. Some experimental results are available on the free-surface aeration of circular water jets (e.g., Heraud, 1966; Ervine and Falvey, 1987; Ruff et al., 1989; Tseng et al., 1992) but there is little information on the free-surface aeration of two-dimensional water jets (see review in Chanson, 1997a).

The present paper describes new experiments performed with two-dimensional water jets discharging into air. Three experimental configurations were used (Fig. 1). It is the purpose of the study to present new experimental evidence of the air-water flow properties in the developing shear layer immediately downstream of the nozzle (i.e., $x/d_o < 20$, where d_o is the nozzle thickness). Altogether the results provide new information on the air entrainment mechanisms, the advective diffusion of air bubbles, the momentum exchange process and the distributions of entrained bubble sizes. Full details of the experimental data were reported in Chanson (1995a), Chanson and Toombes (1997), and Chanson and Brattberg (1997).

Experimental Apparatus

Experimental Channels. Three experimental configurations of two-dimensional water jets were used at the University of Queensland (Fig. 1, Table 1). Experiment No. 1 is basically a water wall jet (0.03 m thick, 0.5 m wide). Experiment No. 2 is an air-water free-shear layer at an abrupt drop ($\Delta z = 0.13$ m, $W = 0.5$ m). The third experiment is a vertical free-falling jet: it consists of a two-dimensional jet issuing from a 0.012 m slot nozzle and discharging downwards. The PVC jet support is 0.35 m long.

The discharge was measured with a Venturi-type device (i.e., Dall™ tube) in experiments No. 1 and No. 2, and with orifice meters in experiment No. 3. The error on the discharge measurement was less than 2 percent.

For experiments Nos. 1 and 2, the vertical probe translation was controlled by a fine adjustment travelling mechanism connected to a Mitutoyo™ digimatic scale unit (Ref. No. 572-503). The error on the vertical position of the probe was less than 0.025 mm and the accuracy on the longitudinal position of the probe was estimated as $\Delta x < 1$ cm. In experiment No. 3, the displacement of the probes in the direction normal to the jet support and along the jet direction were controlled by two fine adjustment travelling mechanisms (made in-house) and the positions were measured with two Lucas Schaevitz Magnarules Plus™ (MRU-012 and MRU-036 in the normal and longitudinal directions, respectively). The error in the longitudinal and normal positions of the probes was less than 0.1 mm in each direction.

Contributed by the Fluids Engineering Division for publication in the JOURNAL OF FLUIDS ENGINEERING. Manuscript received by the Fluids Engineering Division August 29, 1997; revised manuscript received July 6, 1998. Associate Technical Editor: M. Sommerfeld.

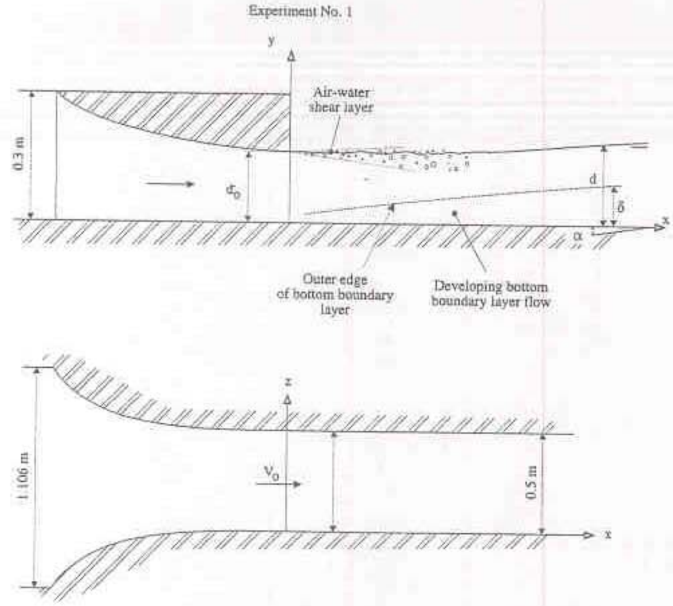

Experiment No. 1

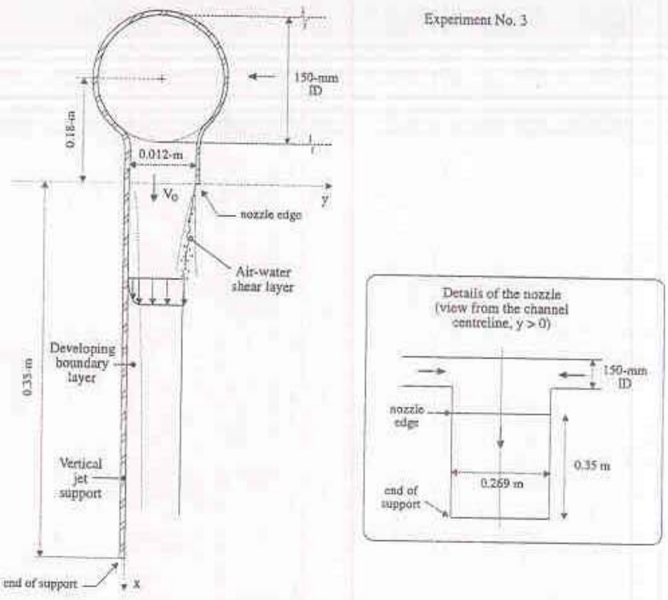

Experiment No. 3

Fig. 1 Sketch of the experiments

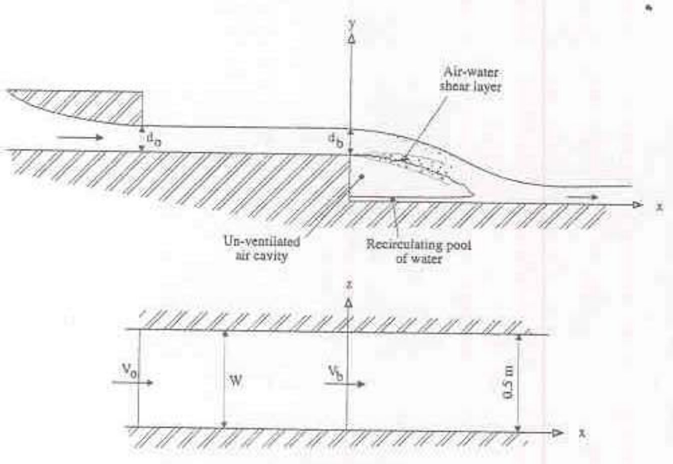

Experiment No. 2

Instrumentation. The air-water flow properties were recorded using two types of conductivity probes made at the University of Queensland, based on an earlier design (Chanson, 1995a, Cummings and Chanson, 1997). A single-tip conductivity probe (inner electrode ∅ = 0.35 mm, outer electrode ∅ = 1.42 mm) was used to perform air concentration measurements only in experiments Nos. 1 and 2.

A two-tip conductivity probe was used to record simultaneously the air concentration, air-water velocity and bubble frequency in experiment No. 3. Each tip is identical with an internal concentric electrode (∅ = 25 μm, platinum electrode). The tip spacing is 8 mm.

Both conductivity probes were excited by an electronic system (air bubble detector Ref. AS25240) designed with a response time less than 10 μs. The measurements were recorded with a scan rate ranging from 10 to 20 kHz per channel.

In addition, clear water jet velocities were measured with a Pitot tube (external diameter ∅ = 3.3 mm).

Discussion. At low void fractions, the air-water mixture consists of air bubbles surrounded continuously by water. At large void fractions, the mixture is predominantly water droplets surrounded by air. For void fractions between 0.3 and 0.7, the flow is a homogeneous mixture but the air-water flow structures are not well understood. In the present study, the writers define an air bubble as a volume of air surrounded continuously or

Nomenclature

C = air concentration defined as the volume of air per unit volume of air and water; it is also called void fraction
ch_{ab} = bubble chord length (m)
$(ch_{ab})_{mean}$ = mean bubble chord length (m)
D_t = turbulent diffusivity (m²/s)
d = jet thickness (m) measured perpendicular to the flow direction
d_o = jet thickness (m) at the nozzle
F_{ab} = air bubble frequency (Hz)
$(F_{ab})_{max}$ = maximum air bubble frequency (Hz) recorded in a cross-section
f_{ab} = dimensionless bubble frequency: $f_{ab} = F_{ab}^{*}\sqrt{x^{*} d_o}/V_o$
g = gravity constant: $g = 9.80$ m/s²
q = volume discharge per unit width (m²/s)
t = dimensionless variable
u = dimensionless variable
V = velocity (m/s)
V_o = mean flow velocity (m/s) at nozzle
W = channel width (m)
X = longitudinal coordinate (m)
x = distance along the flow direction (m)
y = distance (m) measured normal to the flow direction
α = angle between the flow direction and the horizontal
Δ = error
Δz = drop height (m)
ρ = density (kg/m3)
μ = dynamic viscosity
∅ = diameter (m)

Subscripts

w = water flow
o = nozzle flow conditions

Table 1 Experimental flow conditions

Ref. (1)	Slope α (deg.) (2)	Deflector and nozzle geometry (3)	Nb of Exp. (4)	V_o (m/s) (5)	d_o (m) (6)	Comments (7)
Experiment No. 1[(a)]	4.0	Elliptical convergent (10:1 contraction in flow thickness and 2.2:1 in jet width).	1	5.0	0.03	Wall jet issued from a smooth convergent nozzle. W = 0.5 m. Single-tip conductivity probe.
Experiment No. 2[(b)]	0	Elliptical convergent (10:1 contraction in flow thickness and 2.2:1 in jet width).	1	5	0.03	Nappe flow at an abrupt drop (Δz = 0.131 m). W = 0.5 m. Single-tip conductivity probe scanned at 8 kHz (for 150 s).
Experiment No. 3[(c)]	89	S-shaped convergent (12.5:1 jet thickness contraction followed by a 50 mm straight section).	7	1.4 to 7.9	0.012	Vertical free-falling jet. W = 0.269 m. Double-tip conductivity probe scanned at 10 kHz (per channel).

Notes: d_o, V_o: initial nozzle thickness and flow velocity; slope: streamline angle with horizontal at nozzle.
[(a)]: data reported in Chanson (1995); [(b)]: data reported in Chanson and Toombes (1997); [(c)] data reported in Chanson and Brattberg (1997).

not by water interfaces. Practically it is an air entity detected by the leading tip of the probe between two consecutive air-water interface events.

Further, the bubble frequency, at a given position $\{x, y\}$ is defined as the number of air bubbles detected by the leading tip of the conductivity probe per unit time.

Experimental Results

Free-Surface Aeration. For all investigated flow conditions (Table 1), substantial free-surface aeration was always observed immediately downstream of the nozzle (Figs. 2 to 4). Figures 2 to 4 present typical distributions of air concentration C, dimensionless velocity V/V_o and dimensionless bubble frequency $f_{ab} = F_{ab}*\sqrt{x*d_o/V_o}$, where x is the distance from the nozzle in the flow direction, y is the distance normal to the jet support, V is the mean air-water velocity, V_o is the nozzle velocity, d_o is the jet thickness at the nozzle and F_{ab} is the air bubble frequency.[1] Note on Fig. 3 that the upper free-surface of the nappe is not a free-shear layer. The upper nappe entrainment process was analyzed and discussed elsewhere (Chanson, 1989).

[1] The air bubble frequency is defined as the number of air bubbles detected by the probe leading tip per second.

In all the experiments, the air concentration distributions follow closely a solution of the diffusion equation:

$$C = \frac{1}{2}*\left(1 - \operatorname{erf}\left(\frac{1}{2}*\sqrt{\frac{V_o}{D_t}}*\frac{y}{\sqrt{x}}\right)\right) \quad (1)$$

where D_t is the turbulent diffusivity, assumed independent of the transverse direction y and the function erf is defined as:

$$\operatorname{erf}(u) = \frac{2}{\sqrt{\pi}}*\int_0^u \exp(-t^2)*dt \quad (2)$$

Equation (1) was developed and validated for two-dimensional free-shear layers by Chanson (1989, 1995). The above result (Eq. (1)) may be extended to the developing flow region of a two-dimensional water jet discharging into the atmosphere. Note that Eq. (1) is not valid when the jet core becomes aerated.

Velocity Distribution. Distributions of mean air-water velocity and bubble frequency for experiment No. 3 are presented in Fig. 4. In the near-flow field (i.e., $x/d_o < 17$), the transfer of momentum from the water jet to the air is negligible and the air-water velocity is not affected by the advective diffusion of air bubbles (Fig. 4). For the free-falling jet experiments, the free-stream velocity satisfied the Bernoulli equation:

$$V = V_o*\sqrt{1 + \frac{2*g*x}{V_o^2}} \quad \text{for} \quad C \le 0.99 \quad \text{and} \quad x/d_o < 17 \quad (3)$$

Note that the developing boundary layer along the jet support was small and could not be detected with the instrumentation.

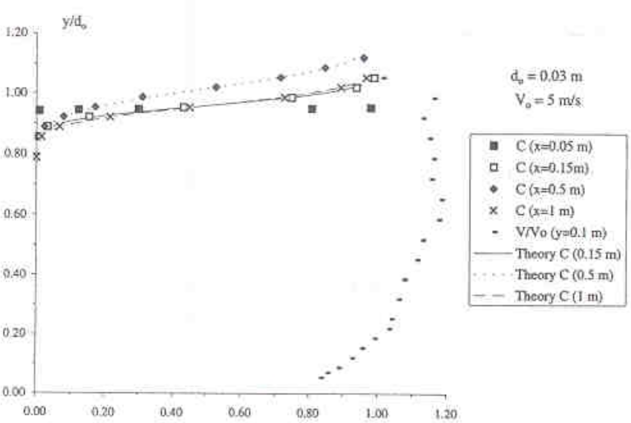

Fig. 2 Air concentration distributions (Experiment No. 1, V_o = 5 m/s, d_o = 0.03 m), comparison with Eq. (1). Uncertainty estimates vert. axis y/do: error = 0.003 (or 0.3%); horiz. axis C: error = 2%; V/Vo error = 5%.

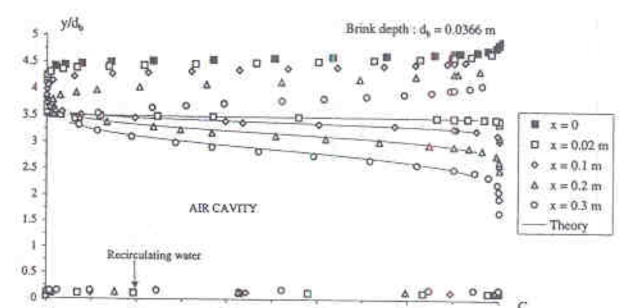

Fig. 3 Air concentration distributions (Experiment No. 2, V_o = 5 m/s), comparison with Eq. (1). Uncertainty estimates vert. axis y/db: error = 0.0017 (or 0.17%); horz. axis C: error = 2%.

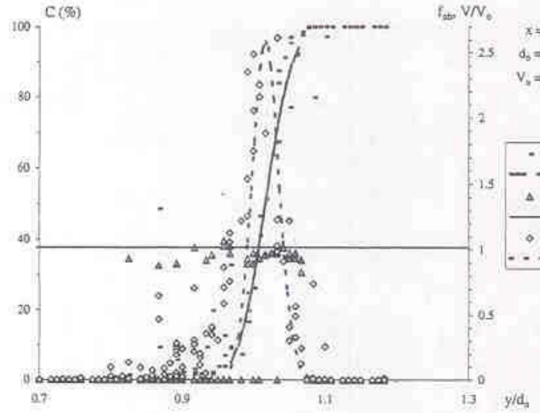

Fig. 4(*a*) $x/d_o = 2.1$

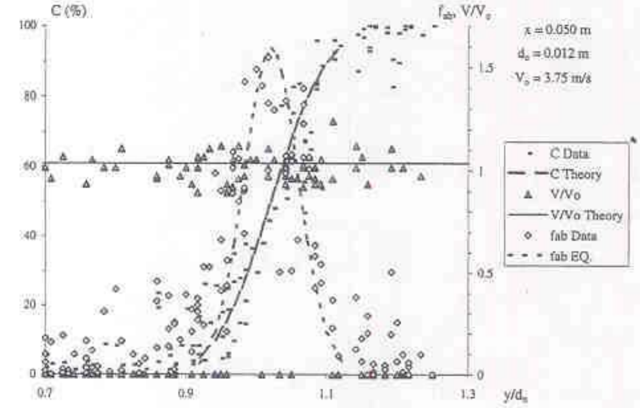

Fig. 4(*b*) $x/d_o = 4.2$

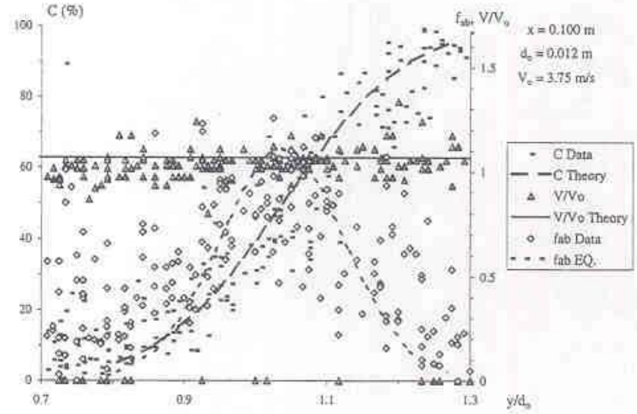

Fig. 4(*c*) $x/d_o = 8.3$

Fig. 4 Air-water flow characteristics in the free-falling jet (Experiment No. 3, $V_o = 3.75$ m/s, $d_o = 0.012$ m): distributions of air concentration C, dimensionless mean air-water velocity V/V_o and dimensionless bubble frequency $f_{ab} = F_{ab}^{*}\sqrt{x^*d_o}/V_o$. Uncertainty estimates horz. axis y/d_o: error = 0.00033 (or 0.033%) vert. axis C: error = 2%; V/vo error = 5%; fab error = 0 (no error on bubble count)

That is, the boundary layer thickness was less than 3.5 mm at $x = 0.2$ m for V_o ranging from 1.4 to 7.9 m/s.

Bubble Frequency. The air bubble frequency distributions exhibit a characteristic shape at each cross-section (Fig. 5). A maximum $(F_{ab})_{\max}$ is observed at about 50 percent air content

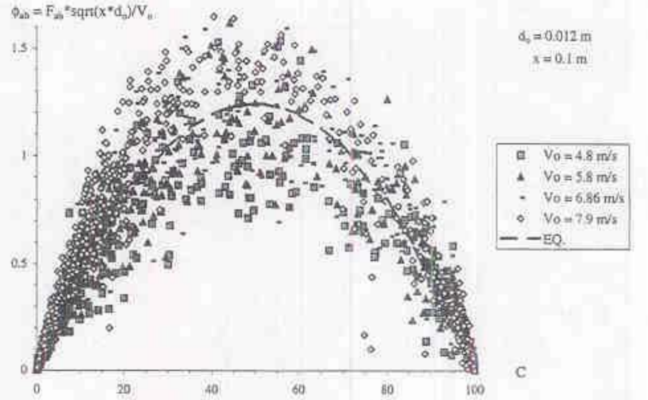

Fig. 5 Dimensionless bubble frequency $f_{ab} = F_{ab}^{*}\sqrt{x^*d_o}/V_o$ as a function of the air content (Experiment No. 3) comparison with Eq. (4). Uncertainty estimates vert. axis fab: error = 0 (no error on bubble count); horz. axis C: error = 2%.

and the bubble frequency tends to zero at very-low and very-large air contents. Overall the dimensionless air bubble frequency distributions are best correlated by a parabolic function:

$$\frac{F_{ab}}{(F_{ab})_{\max}} = 1 - 4^*(C - 0.5)^2 \qquad (4)$$

For the experiments, the dimensionless maximum bubble frequency $((F_{ab})_{\max}{}^*\sqrt{x^*d_o/V_o})$ was observed to be independent of the jet velocity and distance from the nozzle. Hence Eq. (4) may be rewritten as:

$$f_{ab} = 1.242^*(1 - 4^*(C - 0.5)^2) \quad \text{for} \quad \rho_w{}^*\frac{V_o{}^*x}{\mu_w} > 1.5E + 5 \qquad (5)$$

where f_{ab} is the dimensionless bubble frequency: $f_{ab} = F_{ab}{}^*\sqrt{x^*d_o/V_o}$. For $\rho_w{}^*V_o{}^*x/\mu_w < 1.5E + 5$, the coefficient of proportionality differs from 1.242 but the bubble frequency distributions follow closely the parabolic shape (i.e., Eq. (4)).

It is worth noting that the same observation (i.e., Eq. (4)) was obtained in fully-developed supercritical flows (Chanson, 1997b), suggesting that the air-water flow structure might be similar.

Chord Length Distributions. Bubble chord length distributions were recorded using the double-tip conductivity probe in experiment No. 3. The data give some information on the characteristic sizes of air bubbles, air pockets, foam bubbles, bubbles in water projections, and air volumes between water projections. The results (Fig. 6) are presented in the form of cumulative bubble chord length distributions, at various positions from the nozzle and for various nozzle velocities V_o. Note that each figure presents the cumulative probability of all the points for $0 < C < 0.90$ at a fixed distance x and, in each figure, the histogram columns represent the probability of a bubble chord length in 0.5 mm intervals: e.g., the probability of a chord length from 2.0 to 2.5 mm is represented by the column labelled 2.5. The last column (i.e., 100 mm) indicates the probability of bubble chord lengths larger than 100 mm. The results (Fig. 6) show the broad spectrum of bubble chord lengths observed at each cross-section: i.e., from less than 0.5 mm to larger than 100 mm. This is observed both in the low air-content region ($C < 0.5$) and in the high air-content region ($0.5 < C < 0.9$). In both regions, the distributions are skewed with a preponderance of small bubble sizes relative to the mean. The probability of bubble chord lengths is the largest for bubble sizes between 0 and 1.5 mm for $C < 50$ percent and between

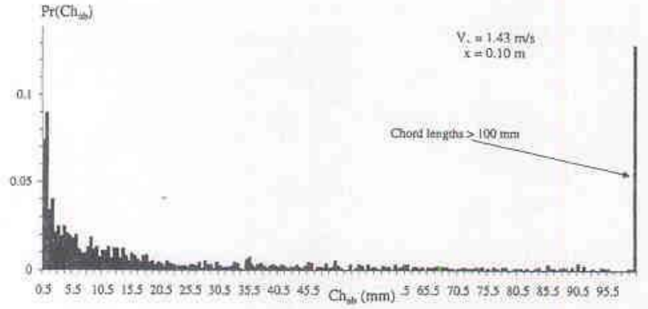

Fig. 6(*a*) $V_o = 1.43$ m/s, $d_o = 0.012$ m, $x = 0.10$ m – chord length interval: 0.5 mm

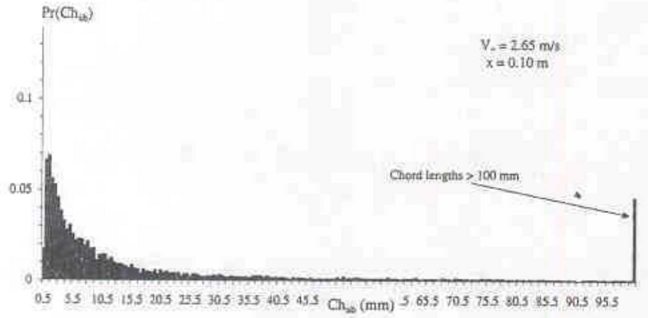

Fig. 6(*b*) $V_o = 2.65$ m/s, $d_o = 0.012$ m, $x = 0.10$ m – chord length interval: 0.5 mm

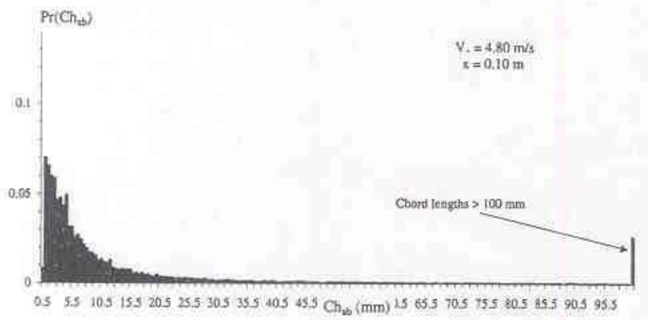

Fig. 6(*c*) $V_o = 4.80$ m/s, $d_o = 0.012$ m, $x = 0.10$ m – chord length interval: 0.5 mm

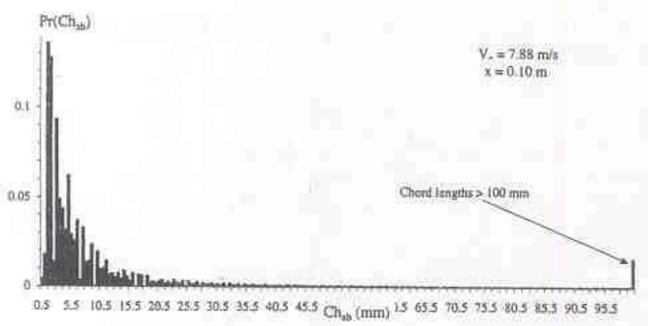

Fig. 6(*d*) $V_o = 7.88$ m/s, $d_o = 0.012$ m, $x = 0.10$ m – chord length interval: 0.5 mm

Fig. 6 Cumulative bubble chord length distributions

0 and 2.0 mm for $0.5 < C < 0.9$. It is worth noting the large amount of bubbles larger than 100 mm. These may be large air packets and air volumes surrounding water structures (e.g. droplets).

For $V_o = 3.75$ m/s, measurements performed at various distances from the nozzle suggest that most entrained air bubbles have small sizes close to the nozzle ($x < 0.1$ m), and that the distributions of chord length are redistributed toward larger sizes further downstream. Note, in any case, the significant amount of large chord length bubbles ($ch_{ab} > 100$ mm).

Discussion

Air Bubble Diffusion. With two-dimensional water jets, the advective diffusion of entrained air bubbles (i.e., Eq. (1)) has been observed with several configurations (see review in Chanson, 1997a, Figs. 2 to 4 in this paper). For all the new experiments, the authors estimated the turbulent diffusivity D_t, satisfying Eq. (1), from the best fit of the data (Table 2). It must be emphasized that the reported values are based on the crude assumption of D_t being independent of the transverse direction y.

Figure 7 presents the dimensionless diffusivity $D_t/(V_o * d_o)$ as a function of the Reynolds number $\rho_w * V_o * d_o/\mu_w$, where V_o and d_o are the characteristics jet velocity and thickness, respectively. The results, presented with logarithmic scales, indicate some scatter suggesting that the Reynolds number might not be the only relevant parameter. Nevertheless, the order of magnitude of the results is consistent with other types of air-water shear flows (see Chanson, 1997a, pp. 216–223). Although the three different experimental geometries (wall jet, free shear layer, free-falling jet) are expected to have different momentum transfer characteristics, the close results of diffusivity coefficients suggest that the air diffusion process is little affected by the geometry and the momentum transfer process.

Note that the data of experiment No. 3 might suggest an increase in dimensionless diffusivity with increasing Reynolds numbers. It is believed that the trend is related to the modification of inflow turbulence with increasing discharge and it is atypical. Experiments Nos. 1 and 2 had both a long smooth-convergent section while the convergent section was very short (i.e., less than 0.2 m) in experiment 3.

Characteristic Bubble Sizes. For any bubble size shape, bubble size distribution and chord length distribution, the mean chord length size (i.e., number mean size) is related to the air content, velocity and bubble frequency by:

$$(ch_{ab})_{\text{mean}} = \frac{CV}{F_{ab}} \tag{6}$$

Equation (6) is mathematically true in bubbly flows (i.e., air bubbles surrounded continuously by water). At the air-water interfaces of high-velocity water jets, Equation (6) is not exactly correct but it still gives an order of magnitude of a characteristic mean bubble size.

Equations (1), (3), (4), and (6) may be combined to deduce the distributions of mean bubble size in the air-water shear flow. For $C < 50$ percent, the mean bubble size (Eq. (6)) is a constant and the order of magnitude is about: $(ch_{ab})_{\text{mean}} \sim 1$ cm. For $C > 0.5$, Eq. (6) predicts a drastic increase of mean chord length with distance from the jet support (or jet centreline) which is consistent with the chord length distribution data.

Conclusion

New experiments have been performed with three types of two-dimensional water jets discharging into air: a wall jet flow, a free shear layer, and a free-falling jet. In each experiment, the distributions of air concentrations follow closely a solution of the diffusion equation (Eq. (1)) and the estimated

Table 2 Air bubble diffusion properties in two-dimensional water jets discharging into air

Ref. (1)	Run (2)	V_o m/s (3)	d_o m (4)	D_t m²/s (5)	$\frac{D_t}{V_o*d_o}$ (6)	X m (7)
Chanson (1988)[a]	860-1	10.71	0.020	1.41E-3	6.58E-3	0.093
	860-2	10.71	0.020	1.55E-3	7.24E-3	0.093
	870-1	10.65	0.032	2.17E-3	6.37E-3	0.199
	870-2	10.65	0.032	1.42E-3	4.17E-3	0.199
	871-1	9.54	0.032	1.50E-3	4.91E-3	0.173
	871-2	9.54	0.032	1.04E-3	3.41E-3	0.173
	872-1	12.01	0.033	2.81E-3	7.09E-3	0.199
	872-2	12.01	0.033	1.71E-3	4.31E-3	0.199
	873-1	8.72	0.031	7.29E-4	2.70E-3	0.146
	873-2	8.72	0.031	8.04E-4	2.97E-3	0.146
	874-1	7.00	0.030	4.52E-4	2.15E-3	0.15
	874-2	7.00	0.030	4.21E-4	2.00E-3	0.15
	1050	7.56	0.035	7.56E-4	2.86E-3	0.153
	1051	10.56	0.035	1.70E-3	4.60E-3	0.391
	880-1	6.21	0.069	3.58E-4	8.35E-4	0.156
	880-2	6.21	0.069	3.36E-4	7.84E-4	0.156
Low (1986)[a]	A7	4.61	0.046	5.58E-4	2.63E-3	0.288
	A8	5.19	0.047	4.86E-4	1.99E-3	0.327
	A9	5.71	0.053	9.99E-4	3.30E-3	0.342
	A10	6.64	0.057	2.93E-3	7.74E-3	0.44
	A11	8.36	0.056	1.63E-3	3.48E-3	0.349
Present study Experiment No. 1	Run P5	5.00	0.030	9.17E-4	6.11E-3	0.15
Experiment No. 2	Q75_St2CL	4.10	0.037	2.56E-3	1.69E-2	0.2
Experiment No. 3	FJ-2-100	1.43	0.012	2.65E-5	1.54E-3	0.1
	FJ-3-100	2.65	0.012	1.06E-4	3.33E-3	0.1
	FJ-4-100	3.75	0.012	2.70E-4	6.00E-3	0.1
	FJ-5-100	4.80	0.012	4.49E-4	7.80E-3	0.1
	FJ-6-100	5.83	0.012	5.03E-4	7.19E-3	0.1
	FJ-7-100	6.86	0.012	8.09E-4	9.83E-3	0.1
	FJ-8-100	7.88	0.012	8.96E-4	9.48E-3	0.1

Notes: X: considered interval (i.e., $0 < x < X$); (a) data reanalyzed by Chanson (1997a).

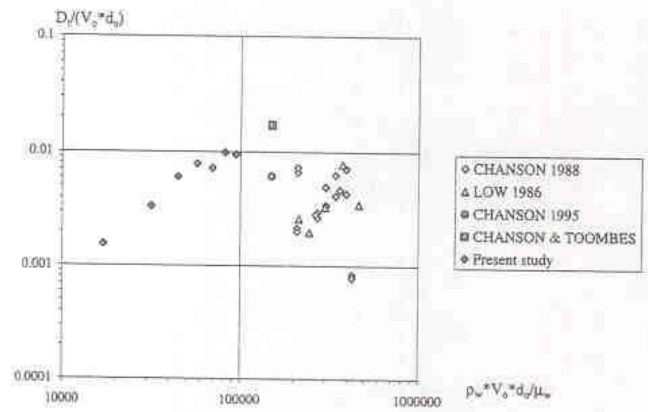

Fig. 7 Dimensionless diffusivity $D_t/(V_o^* d_o)$ as a function of the Reynolds number $\rho_w * V_o * d_o / \mu_w$ (Table 2)

turbulent diffusivity coefficients are of a similar order of magnitude. In experiment No. 3, the velocity and bubble frequency distributions were recorded also. Bubble chord length data show a wide range of entrained bubble sizes (from 0 to over 100 mm chord length). The relationship between the void fraction and the bubble frequency is a parabolic law (Eq. (4)), identical to that observed in self-aerated open channel flows.

Further experiments are necessary to extend the range of flow conditions as well as to investigate the interaction between the momentum shear flow and the air diffusion process.

Acknowledgments

The authors want to thank particularly Professor C. J. APELT, University of Queensland who supported this project since its beginning. They acknowledge the support of the Department of Civil Engineering at the University of Queensland which provided the experimental facility and the financial support of Australian Research Council (Ref. No. A89331591). The first and third authors were supported by Postgraduate scholarships sponsored by the Australian Research Council and the University of Queensland, respectively.

References

Chanson, H., 1988, "A Study of Air Entrainment and Aeration Devices on a Spillway Model." Ph.D. thesis, Ref. 88-8, Dept. of Civil Engrg., University of Canterbury, New Zealand.

Chanson, H., 1989, "Study of Air Entrainment and Aeration Devices." *Journal of Hydraulic Research*, IAHR, Vol. 27, No. 3, pp. 301–319.

Chanson, H., 1995, "Air Bubble Entrainment in Free-surface Turbulent Flows. Experimental Investigations." Report CH46/95, Dept. of Civil Engineering, University of Queensland, Australia, June, 368 pages (ISBN 0 86776 611 5).

Chanson, H., 1997a, *Air Bubble Entrainment in Free-surface Turbulent Shear Flows*, Academic Press, London, UK, 401 pp.

Chanson, H., 1997b, "Air Bubble Entrainment in Open Channels. Flow Structure and Bubble Size Distributions." *International Journal of Multiphase Flow*, Vol. 23, No. 1, pp. 193–203.

Chanson, H., and Brattberg, T., 1997, "Experimental Investigations of Air Bubble Entrainment in Developing Shear Layers," Report CH48/97,

Dept. of Civil Engineering, University of Queensland, Australia, Oct., 309 pp.
Chanson, H., and Toombes, L., 1997, "Flow Aeration at Stepped cascades," Research Report No. CE155, Dept. of Civil Engineering, University of Queensland, Australia, June, 110 pp.
Cummings, P. D., and Chanson, H., 1997, "Air Entrainment in the Developing Flow Region of Plunging Jets. Part 2 Experimental." ASME JOURNAL OF FLUIDS ENGINEERING, Vol. 119, Sept.
Ervine, D. A., and Falvey, H. T., 1987, "Behaviour of Turbulent Water Jets in the Atmosphere and in Plunge Pools," *Proc. Instn Civ. Engrs., London*, Part 2, Mar. Vol. 83, pp. 295–314. Discussion: Part 2, Mar.–June 1988, Vol. 85, pp. 359–363.
Heraud, D., 1966, "Dispersion des Jets Liquides; Influence des Rugosités de Paroi," ('Dispersion of Liquid Jets: Influence of the Wall Roughness.') Ph.D. thesis, University Grenoble 1, France (in French).
Low, H. S., 1986, "Model Studies of Clyde Dam Spillway aerators." Research Report No. 86-6, Dept. of Civil Eng., Univ. of Canterbury, Christchurch, New Zealand.
Tseng, L. K., Ruff, G. A., and Faeth, G. M., 1992, "Effects of Gas Density on the Structure of Liquid Jets in Still Gases." *AIAA Journal*, Vol. 30, No. 6, pp. 1537–1544.

ASME International Announces . . . The Fifteenth ASME Freeman Scholar Program in Fluids Engineering

ASME International announces the Fifteenth Freeman Scholar Program, applications for which are due by August 1, 1999.

A person of high capability and considerable experience in an area of fluids engineering will be selected as the Freeman Scholar. He/she will be expected to make a major review of a coherent topic in his/her specialty, prepare a comprehensive statement of the state of the field, and suggest key research needs for the future. After suitable review, the results will be presented publicly at the ASME International Mechanical Engineering Congress & Exposition under the auspices of the Fluids Engineering Division, and published in the ASME *Journal of Fluids Engineering*.

The recipient may be from industry, government, education, or private professional practice. He/she need not be a member of ASME.

The honorarium for preparing the review, producing a manuscript in a form for publication and presenting the results at the Congress is $7,500. There will be an additional allowance to cover the cost of travel to the International Mechanical Engineering Congress & Exposition in the year 2000.

The Scholar shall be available, as far as personal commitments permit, for presentation of the lecture at sites of fluids engineering activity in industry, government, or education that so request. In each case, the inviting institution will be expected to bear all expenses and, if necessary, to provide a reasonable honorarium.

Applications for the year 2000 Scholarship are to be submitted in quadruplicate by August 1, 1999. The applicant should send one copy to each member of the Standing Committee listed below and one copy to the ASME Committee on Honors (Three Park Avenue, New York, NY 10016-5990). The application shall include:

(1) The applicant's qualifications for undertaking a major study in the field selected.

(2) A statement of the basis for believing that a summary of the state of the art on the proposed topic will make a significant and timely contribution to current or future real problems in fluids engineering practice.

(3) A description of the ideas to be considered and some of the technology to be reviewed.

A complete statement of qualifications and selection criteria can be obtained from the Chair of the Standing Committee.

The applicant shall arrange also for at least three persons to submit supporting letters before August 15, 1999, directly to the Standing Committee members and to the ASME Committee on Honors. These should be persons who are qualified to judge the technical capabilities of the applicant in the proposed review area and the technical value of the area.

The following are the three most recent Freeman lectures:

- 1998 "The Fluid Mechanics of Microdevices," Mohamed Gad-el-Hak, *Journal of Fluids Engineering*, to be published.
- 1996 "Physics of Forced Unsteady Separated Flows," Kirti N. Ghia, *Journal of Fluids Engineering*, to be published.
- 1994 "Particle Dispersion in Flowing Gases," David E. Stock, *Journal of Fluids Engineering*, published in March 1996.

The Scholar will be designated by December 1, 1999. The draft manuscript, to be completed by September 15, 2000, should not exceed 120 double-spaced manuscript pages, or 30 journal pages, without special permission. The presentation will be made at the 2000 Congress in Orlando, Florida. The final manuscript shall be due one month following presentation to allow an opportunity to incorporate discussion from the Congress.

STANDING COMMITTEE FOR FREEMAN SCHOLAR PROGRAM

Chair:
C. T. Crowe
Department of Mechanical Engineering
Washington State University
Pullman, WA 99164-2920

M. L. Billet
Applied Research Laboratory
The Pennsylvania State University
Box 30
State College, PA 16804-0030

R. A. Bajura
National Research Center for Coal and Energy
West Virginia University
Morgantown, WV 26506-6064

THE FREEMAN SCHOLAR PROGRAM

The Freeman Scholar Program is supported by the ASME Freeman Fund established in 1926 by John R. Freeman, noted Hydraulic Engineer and Scholar, Honorary Member and Twenty-fourth President of ASME. Mr. Freeman suggested a flexible program for utilization of the funds. In early years it supported fellowships for the study of hydraulic laboratory practice in Europe, later it supported publication of important hydraulic research data, and more recently it was granted to support research programs in hydraulics and fluid mechanics. The Freeman Scholar Program in fluids engineering represents a timely usage of the Fund and is consistent with the intentions of the donor.